論文 / 著書情報
Article / Book Information

論題(和文)	
Title(English)	VIBRATION CONTROL OF HIGH-RISE BUILDING USING PASSIVE-BASE ISOLATION AND ACTIVE CONTROL
著者(和文)	宮本 皓, 佐藤 大樹, 余 錦華
Authors(English)	Kou Miyamoto, Daiki Sato, Jinhua She
出典(和文)	, , ,
Citation(English)	Proceedings of 3nd Joint Workshop on Building / Civil Engineering between Tongji & Tokyo Tech, , ,
発行日 / Pub. date	2016, 8

3nd Joint Workshop on Building / Civil Engineering between Tongji & Tokyo Tech
August 2-4, 2016, Tokyo Institute of Technology, Yokohama, japan

VIBRATION CONTROL OF HIGH-RISE BUILDING USING PASSIVE-BASE ISOLATION AND ACTIVE CONTROL

Kou Miyamoto[1] , Daiki Sato[2], and Jinhua She[3]

1) Ph.D. candidate, Department of Architecture and Building Engineering, Tokyo Institute of Technology, Yokohama, Japan
2) Associate professor, Laboratory for Future Interdisciplinary Research of Science and Technology (FIRST) , Tokyo Institute of Technology, Yokohama, Japan
3) Professor, Department of Mechanical Engineering, Tokyo University of Technology, Hachioji, Japan

Abstract: This paper compares the control performance of a base-isolated building and that when active structural control (ASC) is installed in the building, and shows that the HSC is more practical than ASC. If a building employs base isolation, the natural period becomes longer. As an effect, the deformation of the base isolation may become longer than that of the allowable. Hence, it is difficult to simply use a base isolation for a high-rise building. This paper uses the combination with ASC and base isolation.

1. INTRODUCTION

In the last a few decades, there are many studies about active structural control (ASC). The first implementation of full-scale ASC was the Kyobashi Center Building in 1989 (B. F. Spencer et al. 2003). Many high-rise buildings have been constructed around the world in the past a few decades. Nowadays, many advanced control strategies are applied for ASC to improve control performance. For example, robust control (ex Yamada et al.1993, Bai at el. 2009 Zhang at el. 2014, Li et al 2014), fuzzy control(ex S. Pourzeynali 2006, Kwan-Soon Park et al. 2015), prediction control (Fall et al. 2006) and adaptive control(Amini et al 2013) are already applied for ASC.

On the other hand, passive structural control (PSC) has been used for many buildings to suppress vibration caused by winds and earthquakes.

If a building employs base isolation, the natural period becomes longer. As an effect, the deformation of the base isolation may become longer than that of the allowable. Hence, it is difficult to simply use a base isolation for a high-rise building. Hybrid structural control (HSC), which combines PSC with ASC, provides us a possible way to solve this problem. However, to our knowledge, there are only very few studies on hybrid control (ex Avila, S.M et al. 2004). Moreover, those studies did not compare the control performance between ASC, PSC, and HSC. So, it is unclear if the HSC is superior to ASC and PSC.

HSC uses less energy to mitigate vibrations of a building than ASC does. So, the HSC is practical.

This paper compares the control performance of a base-isolated building and that when ASC is installed in the building, and shows that the HSC is more practical than ASC.

2. MODEL OF BASE-ISOLATED *N*-STORY STRUCTURE

This study uses an *N* degree-of-freedom (DOF) shear building mode (Sato et al. 2014). Let T_u be the natural period of the first mode. Then, the height of the building is given by

$$H = T_u / 0.02. \tag{1}$$

Let the damping of the first mode be ξ, and the stiffness of the *i*-th story, k_i (i = 1,…,*N*), is given by

$$\begin{cases} k_1 = \dfrac{{}_s\omega^2 \times m_1 \times {}_s\phi_1 + k_2\left({}_s\phi_2 - {}_s\phi_1\right)}{{}_s\phi_1}, \\ k_i = \dfrac{{}_s\omega^2 \times m_i \times {}_s\phi_i + k_{i+1}\left({}_s\phi_{i+1} - {}_s\phi_i\right)}{{}_s\phi_i - {}_s\phi_{1-1}}, \\ \qquad i = 2,3,\ldots,N-1, \\ k_N = \dfrac{{}_s\omega^2 \times m_N \times {}_s\phi_N}{{}_s\phi_N - {}_s\phi_{N1-1}}, \end{cases} \tag{2}$$

where ${}_s\omega$ is the *s*-th natural frequency, ${}_s\phi_i$ is the *s*-th natural mode, *N* is number of the stories, and m_i is the mass of the *i*-th floor. A isolated base is attached at the basement floor of the *N*- DOF building. Let the density of the base be ρ_b, the damping ratio for the period of base be ξ_b, the period of base be T_f, and the mass of the base be m_b.

The stiffness, K_b, and the damping factor, C_b, of the base are given by

$$K_b = \frac{4\pi^2 (m_b + m_s)}{T_f}, \tag{3}$$

$$C_b = 2\xi_b \sqrt{(m_b + m_s) K_b}, \tag{4}$$

where m_s is the total mass of the N-DOF building.
The dynamics of the N-story building are described by

$$\begin{aligned}&[M][\ddot{x}(t)]+[D][\dot{x}(t)]+[K][x(t)]\\&=-[M]\{1\}[\ddot{x}_g(t)]+[E_u][u(t)]\end{aligned}. \quad (5)$$

where $[x]$ is the vector of displacement of each story; $[M]$ is the mass matrix; $[D]$ is the damping factor matrix; $[K]$ is the stiffness matrix; and $[E]$ is the input matrix for $u(t)$ when ASC is applied, otherwise, it is zero

The state-space representation of (5) is

$$\begin{cases}\dot{z}(t)=Az(t)+Bu(t)+B_d\ddot{x}_g(t),\\ y(t)=Cz(t),\end{cases} \quad (6)$$

where

$$z(t)=\begin{bmatrix}x^T(t) & \dot{x}^T(t)\end{bmatrix}^T,$$

$$A=\begin{bmatrix}0 & I_n\\ -M^{-1}K & -M^{-1}D\end{bmatrix},$$

$$B=\begin{bmatrix}0\\ -M^{-1}E_u\end{bmatrix},\ B_d=\begin{bmatrix}0\\ -E\end{bmatrix},\ C=I_n,$$

$$E=-\begin{bmatrix}1\\1\\\vdots\\1\\1\end{bmatrix},\ E_u=\begin{bmatrix}0 & & & & e_n\\ & & & e_{n-1} & -e_n\\ & & \iddots & \iddots & \\ & e_2 & -e_3 & & \\ e_1 & -e_2 & & & 0\end{bmatrix},$$

where $e_i = 1$ if an ASC device is installed at the i-th story, otherwise, $e_i = 0$ ($i = 1, \ldots, N$).

In (6), C is the output matrix, $y \in R^P$ is the measured output of the system, and E_u is the control input matrix determined by the placement of the active structural controller.

3. DESIGN OF ASC SYSTEM

A state-feedback controller

$$u(t)=Fz(t) \quad (7)$$

is considered in this paper. The block diagram of the ASC system is shown in Fig. 1.Note that $F = 0$ if the ASC is not applied.

This study designed the controller using the linear quadratic regulator (LQR) method, which has been used in many ASC systems. (A. Preumont et al. 2008).

The following performance index

$$J=\int_0^\infty\left\{z^T(t)Qz(t)+u^T(t)Ru(t)\right\}dt \quad (8)$$

has been widely used in the design of an LQR controller. In (8), $Q > 0$ and $R > 0$ are weighting matrices. F is given by

$$F=-R^{-1}B^TP, \quad (9)$$

where P is a positive symmetrical solution of the Ricatti equation

$$A^TP+PA-PBR^{-1}B^TP+Q=0. \quad (10)$$

Note that this design does not take the absolute acceleration or the story drift into consideration, even they are important for the ASC of civil structures.

In contrast, this study considered an LQR controller that minimizes the absolute acceleration and the story drift.

First, let Φ be a linear transformation matrix that

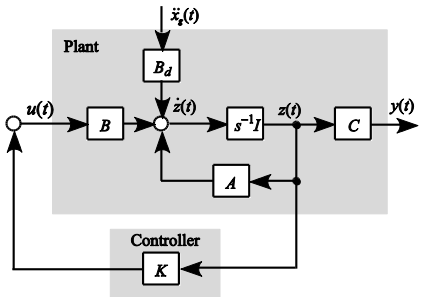

Figure 1. Block diagram of ASC system, (6) and (7).

transforms q (t) into x (t), the vector of the story drift of each story

$$x(t)=\Phi q(t), \quad (11)$$

$$q(t)=\begin{bmatrix}x_N-x_{N-1}\\ \vdots\\ x_2-x_1\\ x_1\end{bmatrix} \quad (12)$$

The following performance indexes J_1 and J_2 that take into consideration story drift and acceleration, respectively, are used:

$$J_1=\int_0^\infty\left\{q^T(t)Q_1q(t)+u^T(t)R_1u(t)\right\}dt, \quad (13)$$

$$J_2=\int_0^\infty\left\{\left[\ddot{x}(t)+\ddot{x}_g(t)\right]^TQ_2\left[\ddot{x}(t)+\ddot{x}_g(t)\right]+u^T(t)R_2u(t)\right\}dt, \quad (14)$$

where Q_1 and Q_2 are weighting matrices for absolute acceleration and story drift, respectively; and R_1 and R_2 are weighting matrices for the control input.

It is clear from (5) that

$$\ddot{x}(t)+\ddot{x}_g(t)=\Psi z(t)+M^{-1}E_uu(t), \quad (15)$$

where

$$\Psi z(t)=-M^{-1}Kx(t)-M^{-1}D\dot{x}(t). \quad (16)$$

Substituting (15) into (14) yields

$$J_2 = \int_0^\infty \left\{ \left[\Psi z(t) + M^{-1}E_u u(t)\right]^T Q_2 \left[\Psi z(t) + M^{-1}E_u u(t)\right] + u^T(t)R_2 u(t) \right\} dt$$

$$= \int_0^\infty \left\{ z^T(t)Q_z z(t) + 2z^T(t)Su(t) + u^T(t)R_3 u(t) \right\} dt. \quad (17)$$

where

$$\begin{cases} Q_z = \Psi^T Q_2 \Psi, \\ S = \Psi^T Q_2 M^{-1} E_u, \\ R_3 = R_2 + E_u^T M^{-T} Q_2 M^{-1} E_u. \end{cases} \quad (18)$$

On the other hand, since

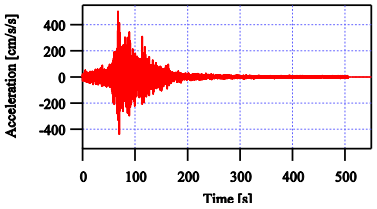

Figure 2. Accelerogram of ART Hachinohe earthquake.

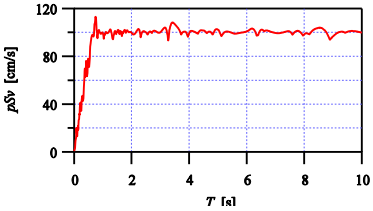

Figure 3. Pseudo velocity of accelerogram in Fig. 2.

$$q(t) = \Phi^{-1}x(t) = \begin{bmatrix} \Phi^{-1} & 0 \end{bmatrix} \begin{bmatrix} x(t) \\ \dot{x}(t) \end{bmatrix}, \quad (19)$$

letting

$$\Xi = \begin{bmatrix} \Phi^{-1} & 0 \end{bmatrix} \quad (20)$$

and substituting (19) and (20) into (13) yields

$$J_1 = \int_0^\infty \left\{ z^T(t)\Xi^T Q_1 \Xi z(t) + u^T(t)R_1 u(t) \right\} dt. \quad (21)$$

This study optimized the following performance index:

$$J_a = J_1 + J_2$$
$$= \int_0^\infty \left\{ z^T(t)Q_a z(t) + 2z^T(t)S_a u(t) + u^T(t)R_a u(t) \right\} dt$$

(21)

where

$$Q_a = Q_z + \Xi^T Q_1 \Xi, \quad S_a = S, \quad R_a = R_1 + R_3. \quad (22)$$

The resulting feedback-control gain is

$$F = -R_a^{-1}\left(S_a^T + B^T P_a\right), \quad (23)$$

where P is a positive symmetrical solution of the Ricatti equation

$$A^T P_a + P_a A - \left(P_a B + S_a\right)R_a^{-1}\left(S_a^T + B^T P_a\right) + Q_a = 0. \quad (24)$$

4. COMPERISON BETWEEN PSC AND HSC

A numerical example is used in this section to compare PSC and HSC.

The accelerogram of ART Hachinohe earthquake was used in this study. For which, the pseudovelocity response spectrum, ${}_pS_v$, is 100 cm/s after 0.64 s. The accelerogram and pseudovelocity response spectrum are shown in Figs. 2 and 3, respectively.

Table 1. Parameters of isolated base for different T_u.

T_u (s)	T_f (s)	ξ_b	ρ_b (kg/m^5)	H (m)
5	8	0.05	2551	250
	6			
3	6			150
	4			
2	4			50

Table 2. Relationship between coefficient of story shear for the first story and parameters of building model.

Model	Coefficient related to control input
Tu=5.0 Tf=8.0	0.081
Tu=5.0 Tf=8.0	0.093
Tu=5.0 Tf=8.0	0.084
Tu=5.0 Tf=8.0	0.104

As for the model of the base-isolated N-story structure, we chose N = 11 (10 stories and an isolated base). T_u was chosen to be 5.0 s, 3.0 s, and 2.0 s for verification. Note that the natural period is relatively long. And the mass of each story was set to be 70000 kg; and the damping of the first mode, ξ, 0.02. The density of the base isolation, ρ_b, damping ratio for the period of base isolation, ξ_b, and the period of base, T_f, are shown in Table 1.

An ASC system was installed at the base-isolated floor. The following weighting matrixes were used to design the controller gain:

$$Q_1 = 10^{\alpha}\begin{bmatrix} 10^2 I_{11} & \\ & I_{11} \end{bmatrix}, \quad Q_2 = 10^{12} \times I_{11}, \quad R_1 = R_2 = 1, \quad (22)$$

and α was chosen to be 12.

4.1 Results of PSC

First, the response of the building with only the base isolation, that is, the PSC, for the accelerogram in Fig. 2 was tested. The results of the peak absolute acceleration,

inter-story-drift angle, and the displacement are shown in Figs. 4-6.

In these figures, NC means that the building does not have the base isolation. Figs. 4-6 show that the introduction of the base isolation reduced the peak absolute acceleration, story drift, and displacement. If T_f becomes longer, the peak displacement will become bigger, and both the peak story drift and the peak acceleration will become smaller.

The simulation results show that displacement of the layer of the isolated base for T_u = 3.0 s and 5.0 s is larger than 60 cm. This shows that it is difficult to use only the base isolation for a building with a long natural period.

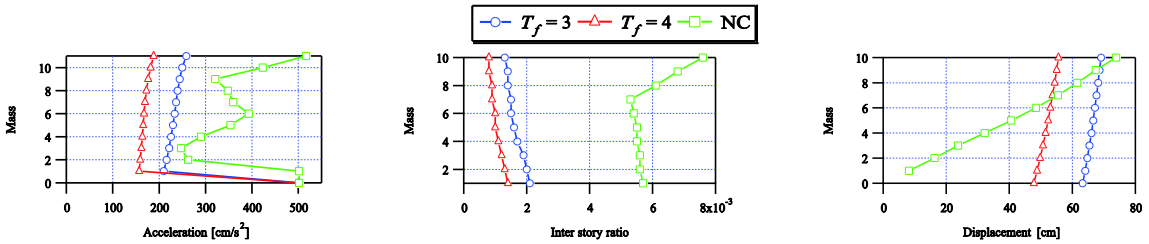

(a) Absolute acceleration (b) Story drift angle (c) Displacement

Figure 4. Peak absolute acceleration, story drift, and displacement for PSC for T_u = 5.0 s.

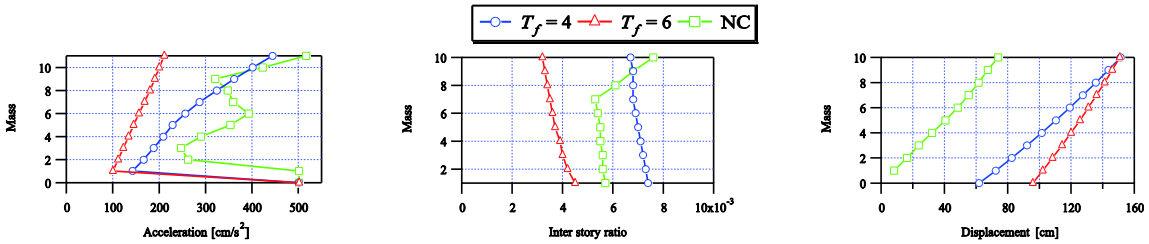

(d) Absolute acceleration (e) Story drift angle (f) Displacement

Figure 5. Peak absolute acceleration, story drift, and displacement for PSC for T_u = 3.0 s.

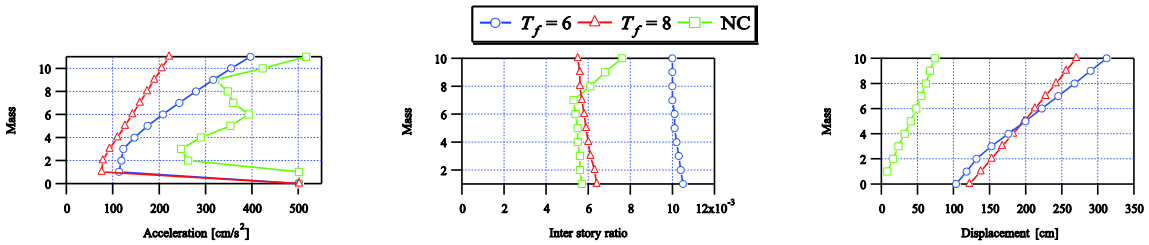

(g) Absolute acceleration (h) Story drift angle (i) Displacement

Figure 6. Peak absolute acceleration, story drift, and displacement for PSC for T_u = 2.0 s.

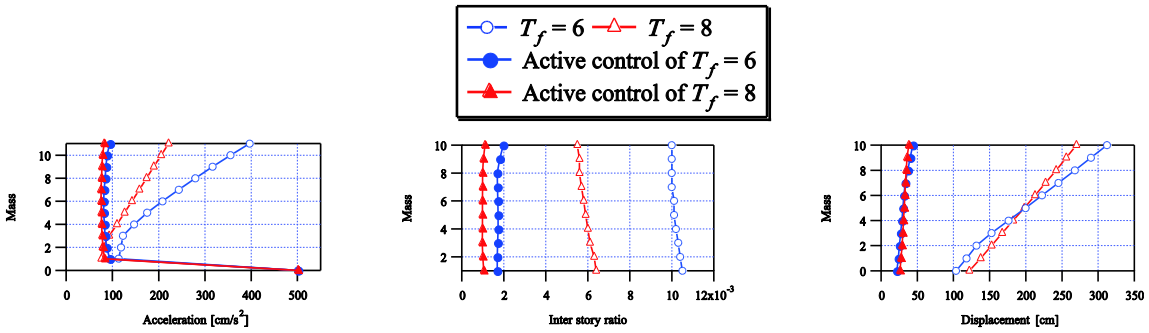

(a) Absolute acceleration (b) Story drift angle (c) Displacement

Figure. 7 Peak absolute acceleration, story drift, and displacement for HSC for T_u = 5.0 s.

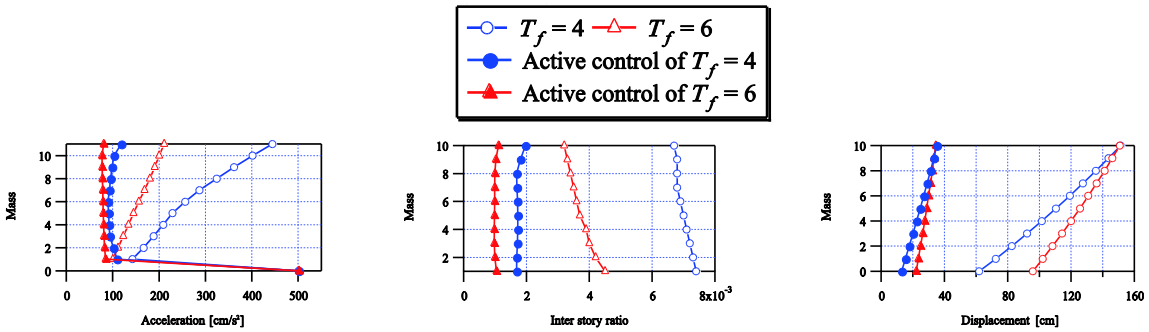

(a) Absolute acceleration (b) Story drift angle (c) Displacement

Figure 8. Peak absolute acceleration, story drift, and displacement for HSC for T_u = 3.0 s.

4.2 Results of ASC

The relationship between the coefficient of the story shear for the first story and the parameters of building model is shown in Table 2.

Figs. 7 and 8 show the simulation results when ASC is combined with PSC.

It is clear from the figures that displacement of the layer of the isolated base was less than 65 cm, and the peak absolute acceleration was also smaller than that for the PSC. More specifically, For T_u = 5.0 s, the largest peak absolute acceleration reduced in 62%; and the largest story drift angle, 80%. And for T_u = 3.0 s, the largest the peak absolute acceleration reduced in 73%;, and the largest story drift angle, 71%.

In addition, the coefficient of the story shear divided by the 2-norm of the control input is less than 0.2. This means that the HSC system suppressed the vibration without giving damage to the structure.

6. CONCLUSION

This paper compares the PSC (base isolation) and HSC (base isolation and ASC). And simulations were carried out for a 11-DOF building model (ten stories with an isolated base) using the accelerogram of Hachinohe earthquake. The following points were clarified:

1) Since the peak displacement of the base-isolated floor was bigger than that allowable, it is difficult to use the PSC for the model with its natural period being 3.0 s or 5.0 s.
2) When the 11-DOF model employed HSC, the peak displacement of the base-isolated floor was less than 65 cm. In addition, compared to the PSC, the peak absolute acceleration for the HSC was reduced in 62% , and the peak story drift for the HSC was also reduced in 86%.
3) The coefficient of the story shear divided by the 2-norm of the control input was less than 0.2. So, the control input was very small and did not damage the structure.

Reference

B. F. Spencer Jr, S. Nagarajaiah (2003), "State of the Art of Structural Control", *JOURNAL OF STRUCTURAL ENGINEERING, American Society of Civil Engineers*, Vol.129(7), p845-856.

Yamada N. Nishitani A. (1993), "AN APPLICATION OF H^∞ CONTROL THEORY TO STRUCTURAL SYSTEMS", *Journal of Structural and Construction Engineering, Architectural Institute of Japan*, No.444, p23-31.

Yuanqiang Bai, Karolos M. Grigoriadis, "Damping parameter design optimization in structural systems using an explicit H∞ norm bound (2009)", *Journal of Sound and Vibration, ELSEVIER*, No.319, p795-806

Hui Zhang, Rongrong Wang, Hunmin Wang, Yang Shi (2014), "Robust finite frequency H∞ static-output-feedback control with application to vibration to active control of structural systems", *Journal of Mechatronics, ELSEVIER*, No.24, p354-366

Zhang Li Sheliang Wang (2014), "Robust optimal H∞ control for irregular buildings with AMD via LMI approach", *Nonlinear Analysis Modeling and Control, Vilnius University*, Vol.19 (2), p256-271.

Kwan-Soon Park, Seung-Yong Ok (2015),"Modal-space reference-model-tracking fuzzy control of earthquake excited structures", *Journal of Sound and Vibration, ELSEVIER*, No.334, p136-150.

S. Pourzeynali, H.H. Lavasani. A.H. Modarayi (2007), "Active control high rise building structures using fuzzy logic and genetic algorithms", Journal of Engineering Structures, ELSEVIER, No.29, p346-357.

Fall Hamed, Sofiane Guessasma, Willy Charon, "Prediction of stability and performance of an active mechanical structure under uncertainty conditions using finite element and neural computation" *Journal of Sound and Vibration, ELSEVIER*, No.28, p1787-1794

Daisuke Sato, Haruyuki Kitamura, Daiki Sato, Toshiaki Sato, Michio Yamaguchi, Naoya Wakita, Yuta Watanuki, "ENERGY BALANCE-BASED SEISMIC RESPONSE PREDICTION METHOD FOR RESPONSE CONTROL STRUCTURES WITH HYSTERETIC DAMPERS AND VISCOUS DAMPERS" *Journal of Structural and Construction Engineering, Architectural Institute of Japan*, No.699, p631-640.